Journal of Sound and Vibration (1998) **217**(3), 523–545
Article No. sv981764

A CRITICAL STUDY OF THE USE OF THE GENERALIZED IMPULSE–MOMENTUM BALANCE EQUATIONS IN FLEXIBLE MULTIBODY SYSTEMS

J. L. Escalona, J. M. Mayo and J. Domínguez

Department of Mechanical Engineering, *University of Seville*,
Camino de los Descubrimientos s/n, 41092 *Sevilla*, *Spain*

(*Received* 5 *February* 1998, *and in final form* 26 *May* 1998)

This paper analyses some aspects of the application of the *generalized impulse–momentum balance equations* to flexible multibody systems. These equations are the result of extending impulsive dynamics to the collision of flexible and constrained bodies. Application of the generalized impulse–momentum balance provides a system of algebraic equations that is solved for the velocity jumps and the impulses associated with the contact force and the reactions involved. As shown in this paper, the physical significance of the *coefficient of restitution*, which is included in the formulation to account for energy losses, can be misinterpreted. The *floating frame of reference approach* was used in combination with the *finite element technique* to describe flexibility and *component mode synthesis* to reduce the number of flexible co-ordinates in the collision problem studied. The number of elastic co-ordinates used to describe flexibility and the time step used in the numerical integration essentially influence the dynamic simulation of the impact process. The underlying message of this research is that the collision simulation entails solving many different balances. However, as shown in this paper, this is not the result of the real phenomenon of succession of impacts. These facts are illustrated with some numerical simulations of impacts of rigid bodies on flexible elements.

1. INTRODUCTION

The generalized impulse–momentum balance equations are the result of applying impulsive dynamics to the collision of flexible bodies in multibody systems. The floating frame of reference approach, jointly with the impulse–momentum balance equations, was applied to rigid body multibody systems by Wehage and Haug [1]. Khulief and Shabana [2] developed the algebraic equation system for multibody systems including rigid and flexible bodies. Flexibility was considered via the finite element method and the component mode synthesis technique was used to reduce the number of flexible co-ordinates. The system was applied to impact on the slider of a slider-crank mechanism, which was assumed to be rigid. Yigit *et al*. [3, 4] used the momentum–balance equations to analyse the impact of a flexible radially rotating beam on a fixed stop. Flexibility was analysed through a continuous

0022–460X/98/430523 + 23 $30.00/0

media approach. The dependence of the coefficient of restitution on the system properties was examined and the numerical results obtained were consistent with experimental data. Palas *et al*. [5] showed that when an infinite set of mode shapes is used, the generalized impulse–momentum balance equations result in a velocity jump only at the contact area between the colliding bodies, other parts of the system remaining at rest. In this case, the generalized impulse of the contact force converges on zero. The transverse impact of a rigid body on a radially rotating beam was studied. The rigid body was artificially removed from the contact area after the first balance was applied. Hsu and Shabana [6], and Gau and Shabana [7], studied the effect of finite rotations on the propagation of impact-induced transverse and axial elastic waves, respectively. Collisions of a rigid solid on a radially rotating beam were simulated through the impulse–momentum balance equations. Again, only a single balance was solved, the impacting rigid body being removed from the impact zone after the balance. The angular velocity of the beam was found to result in additional dispersion of elastic waves. Hwang and Shabana [8] carried out a similar study; however, the rigid body remained stuck to the rotating beam after colliding. The change in system topology was solved by using a different set of mode shapes after the impact. Geometrical stiffening of the beam by effect of the angular velocity was analysed. Yigit and Christoforou [9] compared the results of transverse impacts of rigid solids on beams using two different approaches. Simulations of impacts involving a continuous elastic-plastic contact force were compared with the results of applying the generalized impulse–momentum balance. The beam model used included the effects of shear deformation and rotary inertia, and mode superposition was used to solve the equations. Unlike the previous authors, Yigit and Christoforou used Poisson's rule rather Newton's rule to define the coefficient of restitution. However, they concluded that both approaches led to equivalent results provided an appropriate coefficient of restitution was used.

The basic assumption in impulsive dynamics is to consider that the period of contact between colliding bodies is so short that the co-ordinates remain unaltered during it. In the floating frame of reference approach, the co-ordinates are divided into reference and flexible co-ordinates. Reference co-ordinates describe the rigid body motion of the frame of reference attached to the solids while flexible co-ordinates account for the flexible degrees of freedom used to simulate elastic deformation in the bodies. The assumption of constant co-ordinates contrasts with the analysis of impact-induced vibrations, which arise from the elastic motion of the flexible bodies during the contact period. However, as shown later on, the equations are still valid because the collision process is solved stepwise (i.e., simulating the impact process requires using several balances). The system configuration changes among balances, thus allowing the flexible co-ordinates to change as well. The number of times that the generalized impulse–momentum balance equations need to be solved to conclude the impact process depends on the number of co-ordinates used to describe flexibility, as well as on the time step employed. As shown below it increases with increasing number of flexible co-ordinates and decreases with increasing time step.

The coefficient of restitution, which is included in the formulation to account for energy losses in the vicinity of the contact area, is difficult to interpret under these conditions. This is easily understood because continuous contact is simulated as a virtual succession of instantaneous impacts. At any such impact, the number and severity of which cannot be controlled in advance, part of the energy is assumed to be lost locally.

This paper analyses some aspects of the application of the generalized impulse–momentum balance equations to flexible multibody systems. The floating frame of reference formulation was used to derive the equations of motion. The finite element procedure was used to model the flexibility of the bodies. Nodal co-ordinates were included as flexible co-ordinates. Alternatively, a set of mode shapes was used to describe impact-induced vibrations in the flexible bodies. This technique, called *component mode synthesis*, was used to reduce the number of co-ordinates.

This paper is organized as follows. The following section illustrates the development of the generalized impulse–momentum balance equations for flexible multibody systems using the floating frame of reference approach. Section 3 explains the phenomenon of succession of impacts through the analytical solution of the axial impact of a rigid body on a flexible fixed-free bar. In section 4, the analytical solution obtained in section 3 is compared with numerical simulations involving the generalized impulse–momentum balance equations. Section 5 illustrates the dynamic simulation of the transverse impact of a rigid body on a radially rotating beam. A summary and conclusions are provided at the end of the paper.

2. GENERALISED IMPULSE–MOMENTUM BALANCE EQUATIONS

The motion of multibody systems comprising both flexible and rigid bodies can be analysed by using the floating frame of reference approach. The Lagrange multipliers technique is used to account for constraints on the co-ordinates, and the finite element method to describe flexibility. The equations of motion are [10]

$$\mathbf{M}\ddot{\mathbf{q}} + \mathbf{K}\mathbf{q} + \mathbf{C}_{\mathbf{q}}^{\mathrm{T}}\boldsymbol{\lambda} = \mathbf{Q},$$

$$\mathbf{C}(\mathbf{q}, t) = \mathbf{0}, \tag{1}$$

where $\mathbf{M}$ and $\mathbf{K}$ are the mass and stiffness matrix of the system, respectively. The vector $\mathbf{C}_{\mathbf{q}}^{\mathrm{T}}\boldsymbol{\lambda}$ represents the reaction forces associated to the constraints $\mathbf{C}(\mathbf{q}, t)$, $\mathbf{C}_{\mathbf{q}}$ being the partial derivative of the constraint equations with respect to the system co-ordinates. The generalized forces $\mathbf{Q}$ include the external generalized forces $\mathbf{Q}_e$, the quadratic velocity terms associated to the centrifugal and Coriolis accelerations $\mathbf{Q}_v$ and the contact forces $\mathbf{Q}^*$ (in case of impact). The system co-ordinates are divided into reference and flexible co-ordinates

$$\mathbf{q} = \begin{bmatrix} \mathbf{q}_r \\ \mathbf{q}_f \end{bmatrix}. \tag{2}$$

Co-ordinates $\mathbf{q}_f$ are the nodal co-ordinates of the finite element method. If the component mode synthesis technique is used instead, then a set of shape functions can be used to represent flexible motion. In this case, $\mathbf{q}_f$ are called *modal co-ordinates*.

By differentiating the constraint equations twice, equation (1) can be written in matrix form as

$$\begin{bmatrix} \mathbf{M} & \mathbf{C}_\mathbf{q}^\mathrm{T} \\ sym & \mathbf{0} \end{bmatrix} \begin{bmatrix} \ddot{\mathbf{q}} \\ \boldsymbol{\lambda} \end{bmatrix} = \begin{bmatrix} \mathbf{Q} - \mathbf{K}\mathbf{q} \\ \mathbf{Q}_c \end{bmatrix}, \tag{3}$$

where $\mathbf{Q}_c$ is a vector resulting from the differentiation.

The time interval $I = [\tau_1, \tau_2]$ over which impact occurs, is assumed to be very short. The reference and flexible co-ordinates are supposed to be constant over it. Integrating the equations of motion at I, and making $I = [\tau_1, \tau_2] \to 0$, yields

$$\mathbf{M}\Delta\dot{\mathbf{q}} + \mathbf{C}_\mathbf{q}^\mathrm{T}\mathbf{H}^\lambda = \left(\frac{\partial l_{ij}}{\partial \mathbf{q}}\right)^\mathrm{T} H,$$

$$\mathbf{C}_\mathbf{q}\Delta\dot{\mathbf{q}} = \mathbf{0}, \tag{4}$$

where $\Delta\dot{\mathbf{q}}$ are the system velocity jumps, $\mathbf{C}_\mathbf{q}^\mathrm{T}\mathbf{H}^\lambda$ are the impulsive reactions associated to the constraints, $(\partial l_{ij}/\partial \mathbf{q})^\mathrm{T}$ is the partial derivative of the normal distance between the nodes in contact during impact with respect to the generalized co-ordinates, and H is the impulse associated with the contact force. An additional equation is needed in order to close the system of equations, viz. the *restitution condition*, which relates the initial and final relative normal velocities of the surfaces that come into contact through the coefficient of restitution (Newton's rule). In this problem, it is written as

$$\dot{l}_{ij}(\tau_1) = -e\dot{l}_{ij}(\tau_2) \Rightarrow \left(\frac{\partial l_{ij}}{\partial \mathbf{q}}\right)\Delta\dot{\mathbf{q}} = -(1+e)\left(\frac{\partial l_{ij}}{\partial \mathbf{q}}\right)\dot{\mathbf{q}}(\tau_1), \tag{5}$$

where e is the coefficient of restitution, a scalar that can take values between zero and unity. By combining equations (4) and (5), and writing them in matrix form, the generalized impulse–momentum balance equations are obtained:

$$\begin{bmatrix} \mathbf{M} & \mathbf{C}_\mathbf{q}^\mathrm{T} & -\left(\dfrac{\partial l_{ij}}{\partial \mathbf{q}}\right)^\mathrm{T} \\ \mathbf{C}_\mathbf{q} & \mathbf{0} & \mathbf{0} \\ \left(\dfrac{\partial l_{ij}}{\partial \mathbf{q}}\right) & \mathbf{0} & \mathbf{0} \end{bmatrix} \begin{bmatrix} \Delta\dot{\mathbf{q}} \\ \mathbf{H}^\lambda \\ H \end{bmatrix} = \begin{bmatrix} \mathbf{0} \\ \mathbf{0} \\ v \end{bmatrix}, \tag{6}$$

where

$$v = -(1 + e)\left(\frac{\partial l_{ij}}{\partial \mathbf{q}}\right)\dot{\mathbf{q}}(\tau_1).$$

Before the collision, any motion is analysed by using equation (2). When contact between solids is detected, integration of the equations of motion (2) is stopped. At that point, the algebraic system of equations (6) is solved to obtain the impulses associated with the contact and the reactions forces as well as the velocity jumps. The last are added to the system velocities and integration of the equations of motion is resumed. Note that the coefficient matrix of equation (6) is equal to the coefficient matrix of the accelerations in the equation of motion (2) plus an additional row and column. Therefore, the computational solution of the system of algebraic equations (6) is straightforward. This is the main reason of the efficiency and easy development of the generalized impulse–momentum balance equations in the analysis of impacts in flexible multibody dynamics. However, very important, not immediately apparent aspects, must be considered in order to apply properly this impact analysis technique to flexible mechanisms as shown below.

3. AXIAL IMPACT OF A RIGID BODY ON A FIXED-FREE BAR. SUCCESSION OF IMPACTS

The equation that governs axial vibrations in a beam is the well-known one-dimensional wave equation. St Venant (Figure 1) solved the axial impact of a rigid body on a fixed-free bar. The solution can be found in many classical books [11–13]. Several assumptions are made about this collision, namely:

(1) The impacting mass is considered to be a single-point rigid body.
(2) The flexible body is linear elastic.
(3) The surfaces in contact are planar and contact stress is uniform throughout.
(4) Friction is neglected.
(5) Lateral inertia due to the Poisson effect is also neglected.

In contrast to impact of compact bodies, where the response is governed by local deformation, the fixed-free bar problem is an example of fully global response of bodies (at least for the flexible bar) during the collision [14]. The elastic waves generated while the bodies are in contact excite the overall geometry of the flexible bar and are reflected back from the clamped end one or more times before the

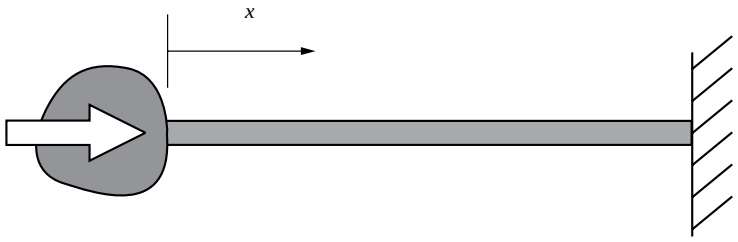

Figure 1. Axial impact of a rigid body on a cantilever beam.

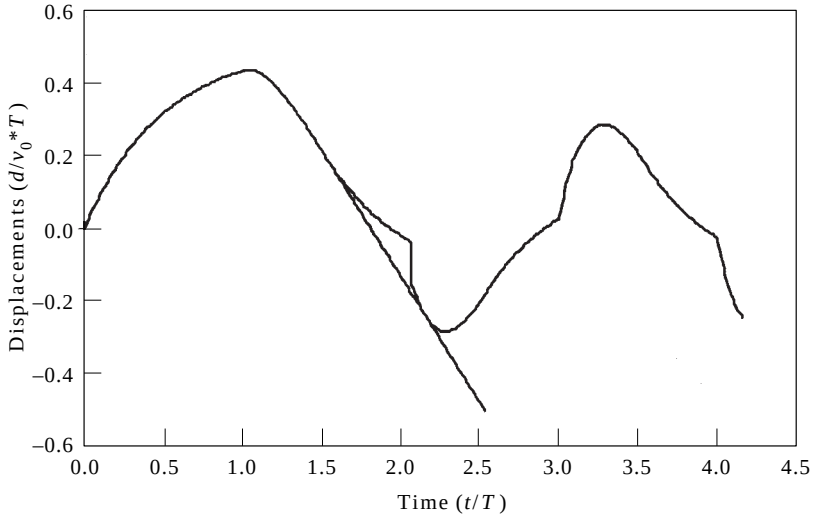

Figure 2. Displacements of rigid body and free-contact section of the beam. Second period of contact. Analytical solution.

process is over. If the fixed-free bar and the rigid impactor have similar masses, then the period of contact is of the same order of magnitude as the period associated with the natural frequency of the flexible body, so use of a *quasi*-static approach is ruled out. Understanding requires analysing wave propagation in the flexible body.

For the particular case of both bodies of identical mass, Escalona *et al*. [15] provided analytical evidence for the phenomenon of succession of impacts. After coming into contact, the impacted surfaces can depart and contact each other again several times before the collision is over. This effect, which is very frequent in transverse impacts on shells, plates and beams, can substantially affect the impact process [16].

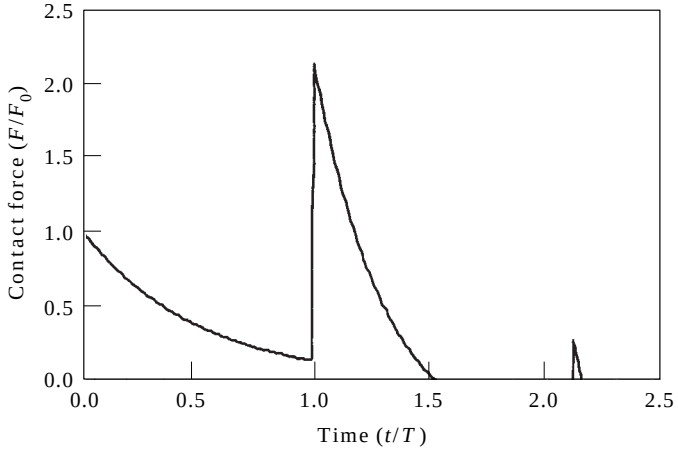

Figure 3. Contact stress. Second period of contact. Analytical solution.

Figures 2 and 3 show the contact stresses and common displacements in the rigid body and the bar contact surface, respectively. As can be seen the collision in the second period of contact is much weaker than in the first. Selected parameter values for this process are as follows:

Initial velocity of the rigid body: v_0
Initial contact stress: $v_0(E\rho)^{1/2}$
Maximum contact stress: $2{\cdot}135\ v_0(E\rho)^{1/2}$ at $t = T$
Duration of the first period of contact: $1{\cdot}534T$
Final velocity of the rigid body after the first period of contact: $-0{\cdot}688\ v_0$
Time interval between first and second period of contact: $0{\cdot}594T$
Initial and maximum contact stress in second period of contact: $0{\cdot}274\ v_0(E\rho)^{1/2}$
Duration of the second period of contact: $0{\cdot}035T$
Final velocity of the rigid body after the second period of contact: $-0{\cdot}692\ v_0$

where E is the modulus of elasticity of the flexible bar, ρ the material density of the bar, $T = 2L(\rho/E)^{1/2}$ the time taken by the elastic waves to travel the length of the bar twice, and L the length of the bar.

As can be inferred from this solution, the second period of contact starts after the rigid body changes the initial direction of its motion. The free section of the beam is accelerated until it collides with the rigid body again. The occurrence of additional contacts may increase the amount of energy lost by virtue of the rigid body motion of the bodies. This is always so judging by the amount of energy lost in local plasticity or friction. However, local effects are not considered in this example. Part of the energy lost through rigid body motion in the first period of contact is recovered in the second one.

4. AXIAL IMPACT OF A RIGID BODY ON A FIXED-FREE BAR. NUMERICAL SIMULATIONS

The problem discussed in the previous section was solved numerically by using the finite element technique to model flexibility in the bar and the generalized impulse–momentum balance equations to solve the collision problem. In order to determine its ability to describe the impact problem, a set of eigenvectors was used as shape functions in the dynamic simulation. In the case of a fixed-free bar, where the flexible body is a structure rather than a mechanism, the method should be called *mode superposition* and not be confused with component mode synthesis. In this case, the shape functions are eigenvectors of its equation of motion, not only admissible shape functions. The solution obtained by using modal co-ordinates is compared with that provided by nodal co-ordinates and both are contrasted with the analytical results.

4.1. SELECTION OF THE COEFFICIENT OF RESTITUTION

The first question that arises in simulating this problem is what coefficient of restitution should be used in the system of algebraic equations. At this point, it is important to note that this selection, needed for correct simulation of the motion using the system of equations (6), is not obvious.

In solving the analytical problem in section 3, it was assumed that the rigid body and the free section of the beam abruptly acquire the same velocity at the beginning of the contact, which of course is physically possible. Because velocity jumps occur as soon as contact starts, a zero relative normal velocity will result in a zero coefficient of restitution. However, using this coefficient does not necessarily mean that any energy is lost as in a rigid body impact. The reason is that the free section has no mass so it abruptly acquires the same velocity as the rigid body without altering the velocity of the rigid body at that instant. However, the system is discretised by assigning a finite mass to the node associated to the free section of the beam. Hence, the use of a zero coefficient would lead to some energy loss at the beginning of the contact. In order to use this approach, one can modify the system configuration during the contact period and model it as one solid in the composite body of a cantilever beam with the mass attached to its end. With this procedure, the simulation would be much more accurate but also more complex.

As in rigid body collisions, the coefficient of restitution can be taken to be the ratio of the initial to the final relative normal rigid body velocities of the solids involved (Newton's rule). From the analytical solution obtained the coefficient turns out to be 0·692. In this case, the coefficient of restitution would characterise the energy lost by the rigid body motion and used in internal vibrations of the flexible beam. However, this number cannot be known in advance because it is one of the solution outputs.

The coefficient to be included in the generalised impulse–momentum balance equations must only characterize the energy lost in local effects such as plasticity because the internal vibrations cannot be assumed to appear instantaneously. In fact, internal vibrations arise from velocity jumps in the flexible co-ordinates, which are obtained from the generalized impulse–momentum balance equations.

Since the local energy lost is neglected a unity coefficient of restitution should be used. Note that, in this case, the rigid body and the free section of the beam will separate instantaneously, and the continuous period of contact is not simulated. As shown in the following sections, the first solution to the momentum–balance equations will not change the direction of motion of the rigid body. This is so because the mass associated to the node in the free section of the bar is much smaller than the rigid body mass. Hence, a new contact will arise during the integration.

4.2. NUMERICAL PROCEDURE

The impact problem was solved numerically by using the finite element procedure. The bar was split into evenly spaced truss elements that possessed axial degrees of freedom only. The Newmark method was used as integration scheme, with $\delta = 0{\cdot}5$ and $\alpha = 0{\cdot}25$ [17]. When mode superposition was adopted, the eigenvectors of the fixed-free bar were used as global shape functions to describe deformation in the bar.

In the numerical simulation, the bar was assumed to consist of steel with a Young's modulus $E = 2{\cdot}1\text{e}11\ \text{N/m}^2$, material density $\rho = 7{\cdot}9\text{e}3\ \text{kg/m}^3$, length $L = 0{\cdot}3$ m, and cross-sectional area $A = 9\text{e-}4\ \text{m}^2$. Also, the concentrated mass was

TABLE 1

Solution of the generalized impulse–momentum balance equations for the axial impact on a cantilever beam

	Rigid body	Free-contact node	Interior node 1	Interior node 2
Initial velocity (m/s)	1	0	0	0
Velocity jump (m/s)	−0·175	1·825	−0·487	0·122
Final velocity (m/s)	0·825	1·825	−0·487	0·122

assumed to be identical to that of the bar, $m = 2{\cdot}133$ kg, and its initial velocity to be $v_0 = 1$ m/s.

4.3. FIRST SOLUTION OF THE GENERALIZED IMPULSE–MOMENTUM BALANCE EQUATIONS

In order to understand what is obtained in the numerical simulations, the first solution of the generalized impulse–momentum balance equations (6) for a unity coefficient of restitution is given in Table 1. In this simple case, the bar was split into three elements. Because the clamped end was modelled by eliminating the degree of freedom associated with it, in the system of algebraic equations (6) there were no constraints, so the equations were simplified. The rows in Table 1 show the initial velocity, velocity jumps and final velocity of all the nodal co-ordinates involved in the analysis.

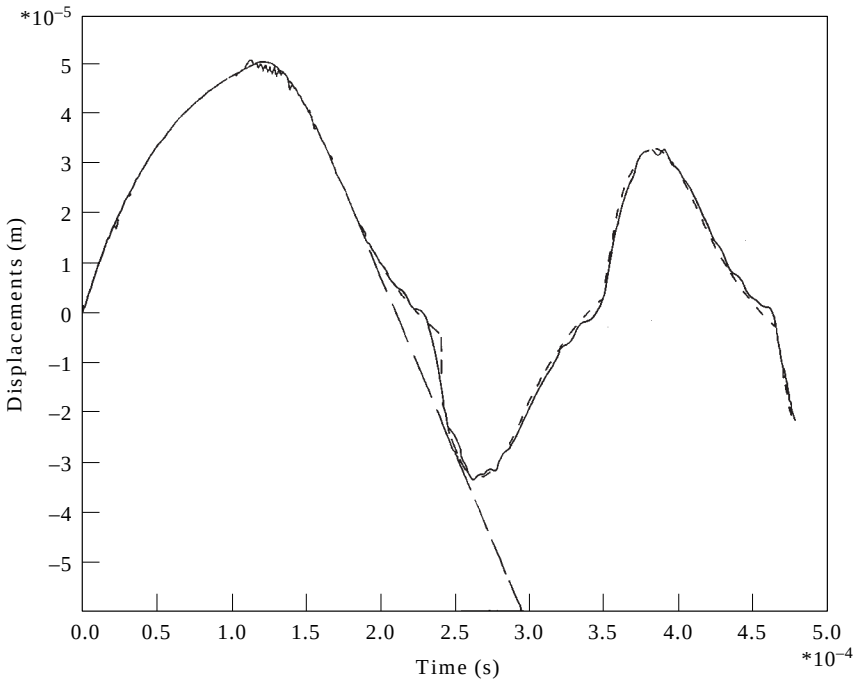

Figure 4. Displacements. 20 Nodes. ——, Free section, numerical result; – – –, free section, analytical result; ——, concentrated mass, numerical result.

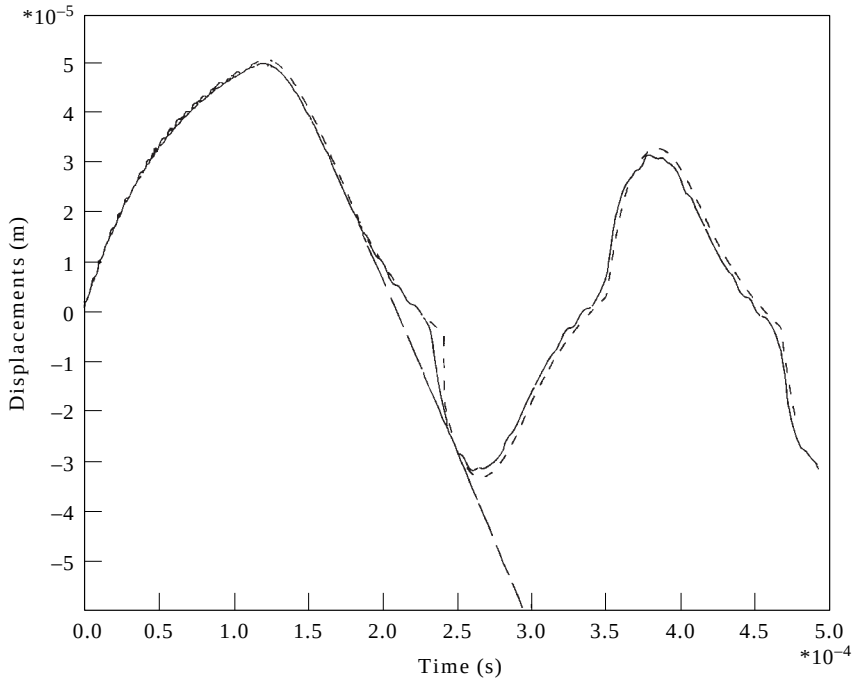

Figure 5. Displacements. 20 Modes. ——, Free section, numerical result; – – –, free section, analytical result; — —, concentrated mass, numerical result.

As can be seen, after the impulse–momentum balance is solved, the rigid body continues to move in the same direction, so, after a few time step intervals it will come into contact with the node associated with the free section again, and new momentum balance will have to be solved then. It is important to emphasize that this succession of balances does not mean a succession of impacts, as shown in

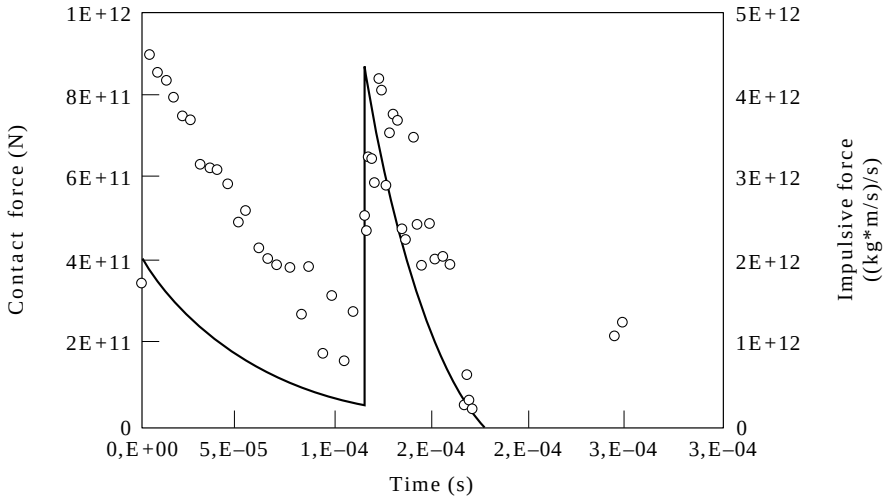

Figure 6. Contact stress from the analytical solution and impulsive forces from the numerical solution (20 modes).

TABLE 2

Influence of the number of flexible co-ordinates

Number of nodes	Duration of impact ($\times 10^{-4}$ s)	Final velocity (m/s)	Number of balances
5	1·56	−0·702	12
10	1·78	−0·715	30
20	(1·82) 2·54	(−0·687) −0·695	63
Exact solution	(1·78) 2·52	(−0·688) −0·692	

TABLE 3

Influence of the coefficient of restitution. Simulations with 20 *mode shapes from* 100 *finite elements*

e	Duration of impact ($\times 10^{-4}$ s)	Final velocity after 2nd period (m/s)	Number of balances
1	(1·71) 2·49	−0·712	49
0·7	(1·80) 2·46	−0·741	296
0·3	(1·86) 2·47	−0·712	338
0	(1·94) 2·46	−0·615	352
Exact solution	(1·78) 2·52	−0·692	

TABLE 4

Influence of the time step. Coefficient of restitution $e = 0$. *Simulations with* 30 *elements*

Time step (s)	Duration of impact (two periods) ($\times 10^{-4}$ s)	Final velocity (m/s)	Number of balances	Energy loss (% of initial energy)
5·89e-7	2·47	−0·42	400	74%
2·95e-7	2·48	−0·58	731	52%
9·82e-8	2·51	−0·75	1954	24%
5·89e-8	2·51	−0·73	3117	16%

discussing the numerical results. The number of balances needed depends on the way the flexible bodies are discretized rather than on the properties of the real body.

Not only the node associated to the free section is dynamically excited after this first balance, as one would expect from the fact that wave propagation starts at this point. However, a larger velocity jump is observed when the node is closer to the contact section.

It has been shown [5] that, the larger the number of flexible co-ordinates used to model a flexible body the smaller is the impulse associated with the contact force, and the closer to the contact zone is the area affected by the velocity jump. This is reasonable because increasing the number of flexible co-ordinates decreases

TABLE 5

Influence of the time step. Coefficient of restitution $e = 0{\cdot}3$. *Simulations with* 30 *elements*

Time step (s)	Duration of impact (two periods) ($\times 10^{-4}$ s)	Final velocity (m/s)	Number of balances	Energy loss (% of initial energy)
5·89e-7	2·47	−0·57	365	54%
2·95e-7	2·48	−0·69	680	34%
9·82e-8	2·51	−0·73	1849	14%
5·89e-8	2·51	−0·72	2907	9%

the mass associated with each degree of freedom (the contact section included). This results in more balances being needed to simulate the complete process and in expectably less severe impacts as the flexible degrees of freedom of the elastic bodies are increased. Here, the severity of the simulated impacts is assimilated to the magnitude of the initial normal relative velocities.

When mode superposition is adopted, if a complete set of eigenvectors is included, then the solution is exactly the same as with nodal co-ordinates and the

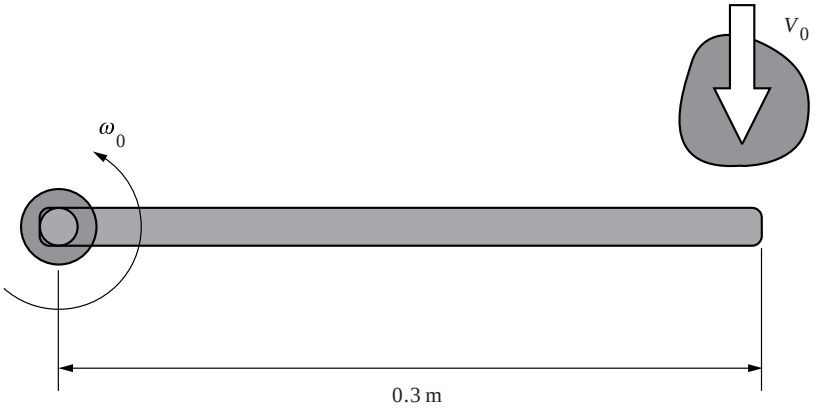

Figure 7. Impact of a rigid body on a radially rotating beam.

TABLE 6

Impulse–momentum balances for the impact on a radially rotating beam

No. of modes	Final velocity (m/s)	Period of balances (s)	No. of balances	Averaged velocity jump (m/s)	ΣM_{ci} (kg m^2/s)	ΣP_{ci} (kg m/s)
5	1·874	$\Delta t = 1{\cdot}53$e-2	15	0·129	8·43e-3	2·78e-1
10	1·786	$\Delta t = 1{\cdot}32$e-2	34	0·054	1·17e-2	1·68e-1
15	1·736	$\Delta t = 1{\cdot}31$e-2	51	0·035	2·2e-3	1·09e-1
Rigid solids	1·943	$\Delta t = 0$	1	2	0·342	2·276

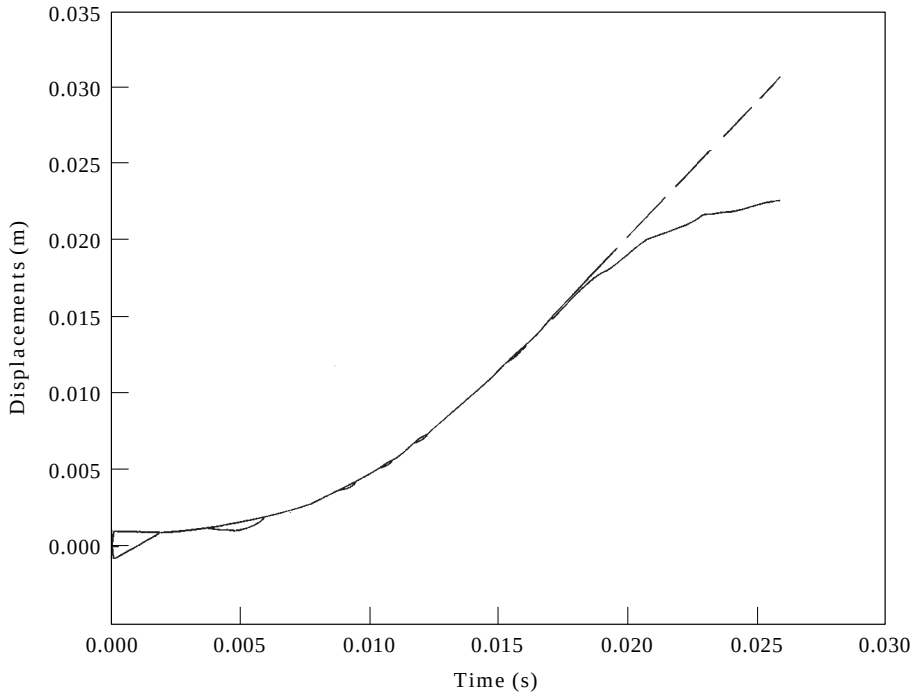

Figure 8. Impact on a radially rotating beam. 10 Modes. ——, Free section; ——, concentrated mass.

equations are equivalent. A different result will be obtained, however, if an incomplete set of eigenvectors is used.

4.4. CONDITIONS FOR IMPACT

The impact logic, i.e., the conditions to be satisfied in order to assume that a new balance must be solved, is described below. A new balance will be solved if both the following conditions, 1 and 2, are satisfied:

(1) penetration: $u_m - u_f \geqslant 0$, and

(2) relative velocities: $v_m - v_f \geqslant 0$

where u_m and v_m are the displacement and velocity of the rigid body; and u_f and v_f are those of the free-contact section of the bar. Our frame of reference is located at the initial position of the rigid body and the positive direction of the x-axis runs towards the clamped end of the bar (Figure 1).

Condition 1 implies that there should be numerical penetration of the bodies. If the degree of penetration found is unacceptably high, then one can use a small number as a tolerated limit to this penetration. If the penetration exceeds the tolerated limit, then the simulation procedure returns to the last integration step and it resumes integration using a smaller time step. However, because the event described occurs over a very short period and the time step used in the simulations is thus very small, the penetration should not be unacceptable. Condition 2 relates the relative velocities. It is satisfied if the rigid body and the free-contact surface are still approaching each other.

4.5. NUMERICAL RESULTS FOR THE IMPACT OF A RIGID BODY ON A FIXED-FREE BAR

Consistency between the analytical solution obtained in section 3 and the numerical simulation with $e = 1$ was in general very good. Figure 4 compares the displacement of the rigid body and the free-contact section of the fixed-free bar as derived analytically and numerically. The numerical problem was solved by using 20 nodes. No second period of contact was detected by this numerical simulation. Because of the low intensity of this impact, the general solution was not substantially modified. Figure 5 shows a similar comparison where the numerical solution was calculated from 20 modal co-ordinates obtained from 100 finite elements. The second period of contact was indeed detected in this case. Therefore, on equal numbers of flexible co-ordinates, the modal approach gives better results. However, modal matrices are quite large and thus use greater amounts of memory and longer CPU times. Using complete sets of eigenvectors led to similar solutions with nodal and modal co-ordinates. However, the modal problem involves more computations to change the co-ordinates.

The generalised impulse–momentum balance equations do not provide the contact forces, but rather the impulses associated to them. Figure 6 shows the analytically obtained contact stress versus the impulses obtained from the balances, divided by the time step. Although they cannot be interpreted to be forces, one can readily see that the intensity of this unreal succession of impacts is related to the instantaneous contact stress of the analytical solution.

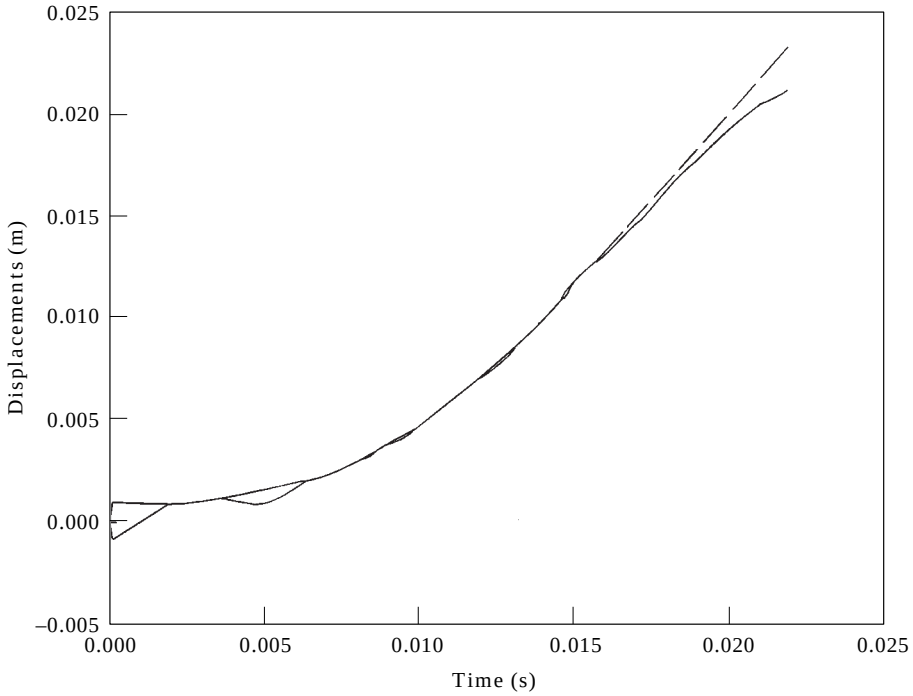

Figure 9. Impact on a radially rotating beam. 15 Modes. ——, Free section; — —, concentrated mass.

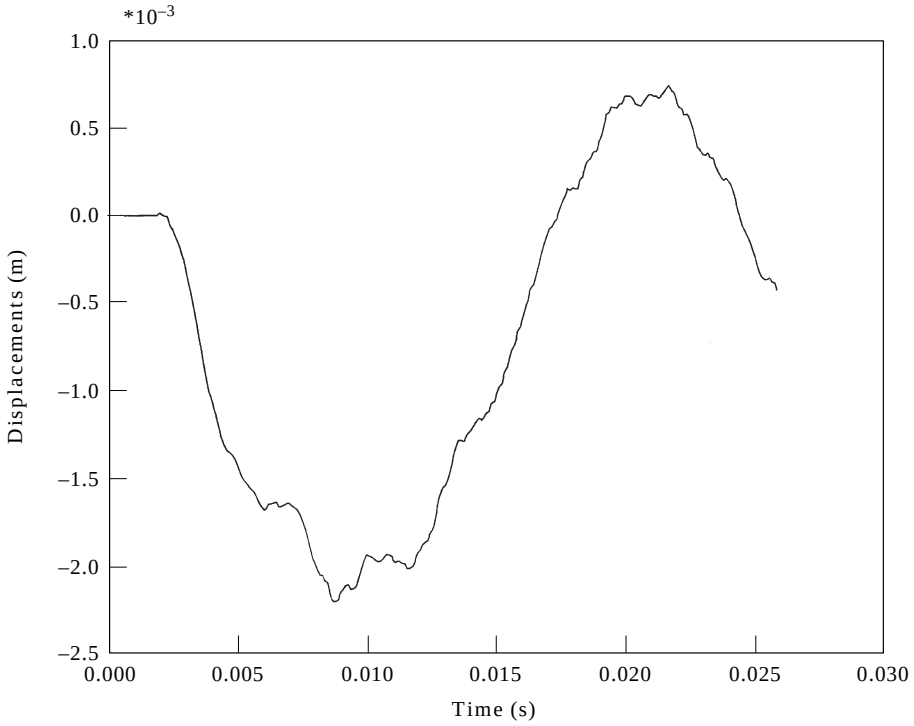

Figure 10. Impact on a radially rotating beam. Elastic displacement of the tip of the beam. 10 Modes.

The number of balances to be solved in order to simulate the complete process depends on the number of flexible degrees of freedom involved. The larger the number of flexible co-ordinates used the smaller will be the mass associated to the node of the free contact surface and hence, the velocity jumps of the free body. More balances will thus have to be solved as the number of flexible (nodal or modal) co-ordinates is increased. This is apparent from Table 2, which gives the number of balances, duration of impact and final velocity for different numbers of flexible degrees of freedom. The duration of impact is approximated by the time interval between the solution for the first and last balances. In cases where a second period of contact was found, the duration of the first and the velocity of the impactor after it are given in brackets.

As explained in section 4·1 a unity coefficient of restitution should be used. However, Table 3 gives the results for several problems that were solved with variable coefficients of restitution smaller than unity in order to analyse its effect. From the results it follows that the number of balances increases as the coefficient of restitution decreases. This is so because the velocity at which contacting nodes separate after any balance decreases as the coefficient decreases, so the nodes can come into new contact faster. One surprising result is that decreased values of the coefficient can result in an increased final velocity of the rigid body. This could never happen in rigid body dynamics. Clearly, the system loses some energy after each balance. If the rigid body has a greater final velocity than in a completely

elastic impact, then all the energy lost will be the energy invested in elastic vibration during the elastic impact. In contrast to the Newtonian concept of the coefficient of restitution in rigid body collisions, the final kinetic energy of the rigid body in the simulation with $e = 0{\cdot}7$ was greater than that in the simulation with $e = 1$, even though in the first simulation the system lost some energy.

Note that, in rigid body dynamics, a zero coefficient of restitution means that the colliding bodies acquire zero relative velocity after the impact. However, when flexible co-ordinates are included, the coefficient means that at once the nodes associated with the contact surfaces acquire the same normal velocity. As soon as elastic forces arise at the node of the free-contact section (not the impactor), it changes its velocity so the nodes can separate and collide again.

Table 4 shows the influence of the time step used to integrate the equations of motion on the impact with a zero coefficient of restitution. From it, one can conclude that a small time step leads to a large number of balances and hence to a high final velocity in the rigid body. This can only be accounted for if the averaged relative velocity of the impacting nodes is much smaller in the balances solved by using smaller time steps. In any case, the influence of the time step is extremely important and its variation results in completely different results. A similar effect is observed when a non-unity coefficient of restitution is used. Table 5 shows the same types of data as Table 4 but obtained with a coefficient of restitution $e = 0{\cdot}3$. As can be seen, the time step is less influential here than in the

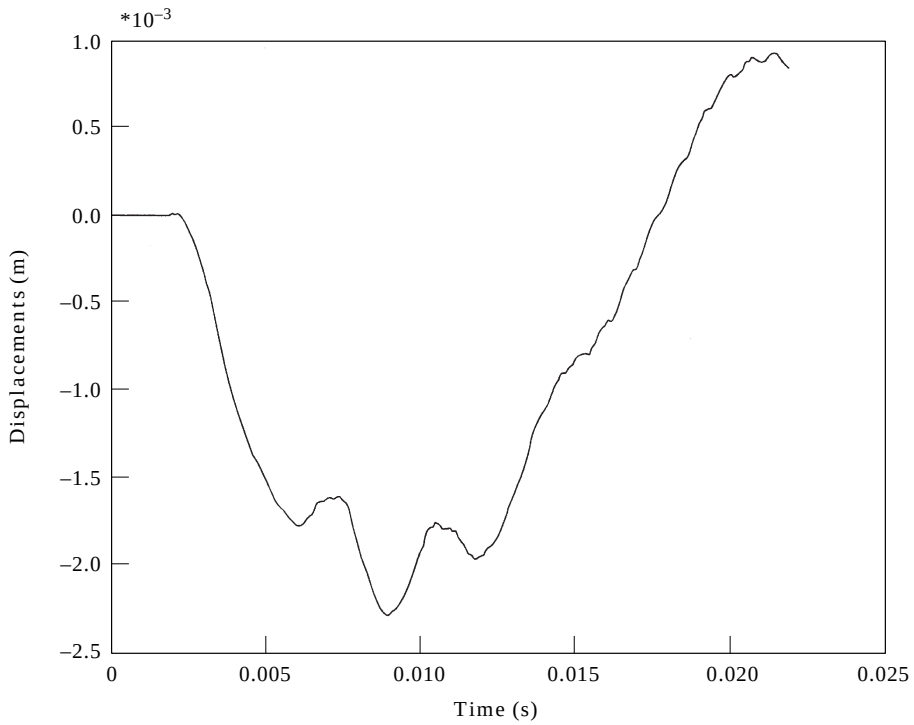

Figure 11. Impact on a radially rotating beam. Elastic displacement of the tip of the beam. 15 Modes.

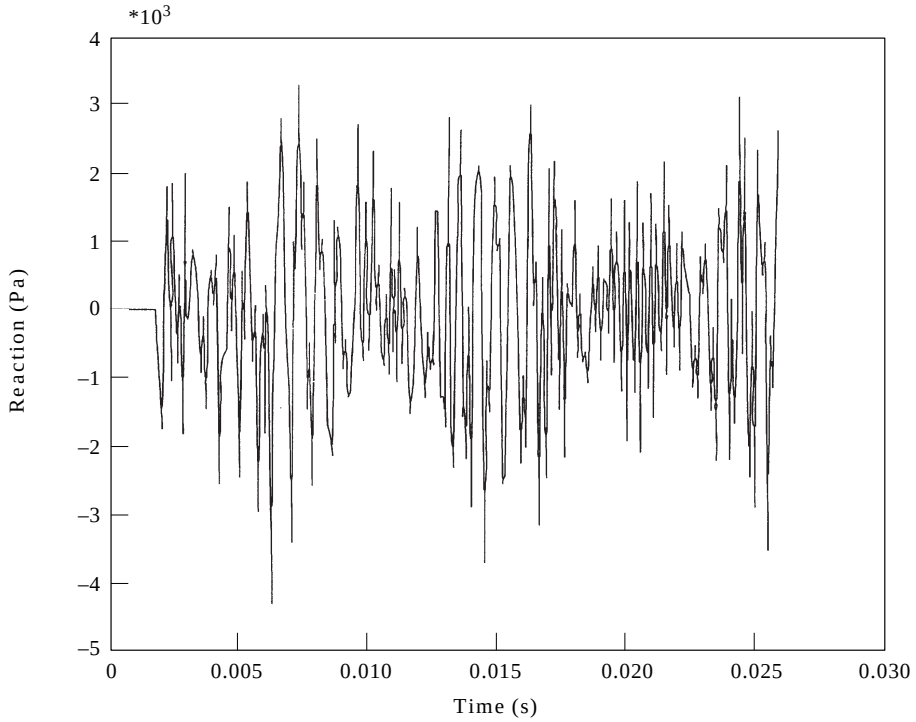

Figure 12. Impact on a radially rotating beam. Vertical reaction at revolute joint. 10 Modes.

simulations with $e = 0$. In general, the differences between the simulations as the time step increases are more important as the coefficient of restitution decreases.

In summary the process simulated by this succession of balances is unrealistic. Clearly, the coefficient of restitution lacks physical significance in this formulation. Consistent results are only guaranteed when the coefficient of restitution is unity (i.e., when no energy is lost). The coefficient of restitution included in the formulation of the generalized impulse–momentum balance equations cannot uniquely characterize the locally lost energy because one cannot control the number of balances needed to conclude the collision or their intensity.

The coefficient of restitution used in all balances of the previous simulations was constant. Some authors [9] use a velocity-dependent coefficient of restitution. The coefficient value is the same as the one that would be obtained for the impact of the rigid impactor with a half-space. Some contact force-indentation law must be adopted to this end. Whether this assimilation is valid is not clear. The previous analysis demonstrates that a balance means neither an impact nor a period of contact. Moreover, the contact section of the flexible body, the mass of which approaches zero as the number of flexible degrees of freedom approaches to infinity, is substituted in this equivalence by an infinite mass (the half-space). Since the separations of the impacting bodies between the balances are physically unreal, it makes no sense to try to find a criterion for using a velocity-dependent coefficient of restitution. This is why a constant coefficient of restitution was used in the previous analysis. Anyway, from results not shown in this paper, the same

conclusions given above are applicable when a velocity-dependent coefficient of restitution is used.

5. IMPACT OF RIGID BODIES ON FLEXIBLE MECHANISMS

This section discusses the numerical simulations of the impact of rigid bodies in flexible mechanisms. In this case, the full system of equations (6) was used (reference co-ordinates and kinematic constraints included). The system was a radially rotating flexible beam that impacted transversally on its free tip (Figure 7). The floating frame of reference approach was used to derive the equations of motion for the flexible mechanism. The Lagrange multipliers associated to the constraint equations were included in the equations of motion to account for the reaction forces. Also component mode synthesis was used to reduce the number of flexible co-ordinates. The equations of motion were integrated by using a variable time step integrator. Simulations were carried out using the general-purpose computer program DAMS [18].

5.1. CONDITIONS FOR IMPACT

The conditions for impact detection must be modified to simulate transverse impacts on beams. In order to allow the flexible co-ordinates to change after each balance, the program integrates a number of time steps after the balance without considering the possibility of a new contact. This is called the "number of calls

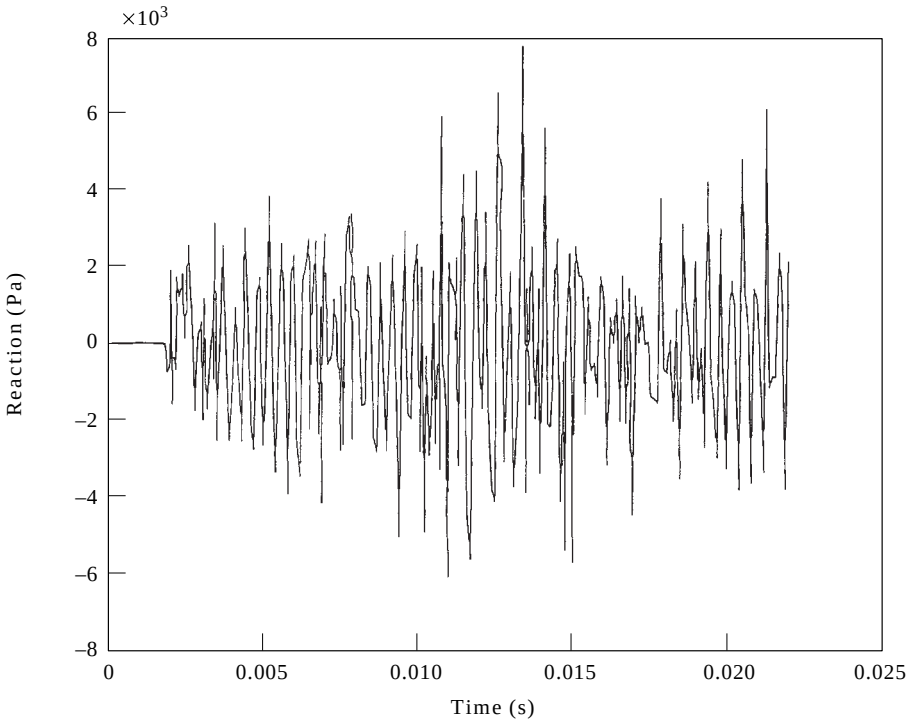

Figure 13. Impact on a radially rotating beam. Vertical reaction at revolute joint. 15 Modes.

after impact''. A small penetration of the solids can occur during this period. Since the beam is modelled as a single line, the rigid body can cross the beam unless the impact logic prevents it.

The algorithm for detecting impacts uses the normal relative distance and velocities of the impacting nodes as variables. They are calculated as follows: the relative normal distance $\mathbf{d}_n$, and normal velocities of the impacting points, $\mathbf{v}_n$, are computed from the relative distance $\mathbf{d}$, and velocity $\mathbf{v}$, and the vector normal to the surface of the flexible beams $\mathbf{n}$. This normal vector is obtained by adding the angle rotated by the frame of reference attached to the flexible beam θ_r to the angle rotated by the node associated to the impacting surface of the beam θ_f

$$\theta = \theta_r + \theta_f, \qquad \mathbf{n} = [-\sin\theta \cos\theta]. \tag{7}$$

Thus, the relative normal distance and velocity are obtained from

$$\mathbf{d}_n = (\mathbf{d} \cdot \mathbf{n})\mathbf{n}, \qquad \mathbf{v}_n = (\mathbf{v} \cdot \mathbf{n})\mathbf{n}. \tag{8}$$

During the computation process, if no balance has yet been solved, an impact is assumed to occur if the relative normal distance between the impacting points is smaller than a low tolerance

$$|\mathbf{d}_n| < tol. \tag{9}$$

At this point, the relative normal velocity $\mathbf{v}_{n0}$ and distance $\mathbf{d}_{n0}$ of the previous time step is stored. In this way, the program stores the initial relative direction of the impact. Obviously, the bodies must eventually separate in opposite relative directions. Additional balances must be solved if both of the following conditions are satisfied:

(1) The actual relative velocity has the same direction as the initial one

$$\mathbf{v}_n \cdot \mathbf{v}_{n0} > 0. \tag{10}$$

(2) The actual relative normal distance has the opposite direction of the initial one

$$\mathbf{d}_n \cdot \mathbf{d}_{n0} < 0. \tag{11}$$

The first condition implies that the surfaces are still approaching and the second one that there is numerical penetration (i.e., contact).

5.2. IMPACT OF A RIGID BODY ON A FLEXIBLE RADIALLY ROTATING BEAM

In this simulation, a flexible beam was supposed to rotate at a constant angular velocity when impacted by a rigid body on its free tip (Figure 7). The following parameters were considered:

Constant angular velocity: 3·142 rad/s
Rigid body initial velocity: $-0{\cdot}0574$ m/s
Relative impact velocity: 1 m/s
Beam mass: 1·138 kg
Rigid body mass: 1·138 kg.

The flexible beam was assumed to consist of steel and to have a rectangular cross section with the following properties:

Young's modulus: 2·1e11 N/m^2

Length: 0·3 m

Cross section: 6 cm $\times$ 0·8 cm.

The beam was split into 15 finite beam elements. Three different models were tested that used 15, 10 and 5 mode shapes to simulate the beam flexibility. Mode shapes were obtained by attaching the body frame of reference rigidly to the revolute joint of the rotating beam. Three, out of the 15 modes used in the simulations were axial modes (viz. the 6th, 10th and 13th). Since the response would be mainly flexural, these three modes had no effect on it. Thus, in practice, it was like using 12, 9 and 5 modes, respectively. All simulations were done with a unity coefficient of restitution.

The results of the generalized impulse–momentum balance equations can be verified by performing some simple calculations. Thus, the rigid body solution for this problem can be obtained from the following system of algebraic equations:

$$\text{Momentum balance: } mv^- + P = mv^+,$$

$$\text{Linear momentum balance: } mv^- L - M = mv^+ L,$$

$$\text{Energy balance: } \tfrac{1}{2}mv^{-2} + M\omega_0 = \tfrac{1}{2}mv^{+2}, \tag{12}$$

where m is the rigid body mass; L is the length of the beam; v^- and v^+ are the initial and final rigid body velocity, respectively; P is the vertical impulsive reaction at the revolute joint; and M is the torque impulsive reaction at the revolute joint needed to maintain its angular velocity constant. Note that because of the constant angular velocity constraint the kinetic conditions of the beam are the same before and after the impact. The third equation above can be substituted by the restitution condition, i.e. one that considers the initial and final relative normal velocities of the impacting points to be identical (with opposite signs). The solution of the system of algebraic equations (12) is

$$v^+ = 1{\cdot}943 \text{ m/s}, \qquad M = 0{\cdot}683 \text{ kg m}^2/\text{s}, \qquad P = 2{\cdot}276 \text{ kg m/s}. \tag{13}$$

Table 6 shows the final rigid body velocity, period of contact (computed as in the simulation of the fixed-free bar), number of balances solved, averaged velocity jump of the rigid body at each balance, and addition of all the impulsive vertical reaction and impulsive torques. The impulses of the reactions at the revolute joint are reduced to the centre of gravity of the beam. These results are given for the three models and compared with the solution of the problem involving rigid bodies. From them, it can be concluded that the more modes are used the smaller is the final velocity of the rigid mass. Increasing the number of flexible degrees of freedom increases the flexibility of the modelled body. The additional mode shapes increase the capacity of the flexible body to store energy in the form of internal vibrations. This energy is taken from the rigid body kinetic energy. The final velocity of the rigid body obtained from the rigid solid solution can be regarded as an upper limit of the final velocity of the rigid body in the flexible body simulation.

Based on the results of the balances, an increasing number of modes increases the number of balances and decreases the velocity jumps and impulsive reactions. The simulated ''periods of contact'' obtained with different models are highly consistent.

Figures 8 and 9 show the global displacement of the rigid body and the free-contact tip of the flexible beam, from the 10-mode and 15-mode solutions, respectively. Figures 10 and 11 show the displacement of the tip of the beam with respect to its body-fixed frame of reference, again with 10 and 15 modes respectively. As can be seen the solution converges as the number of modes is increased. Although the period of contact was simulated in a discrete succession of balances, the results are seemingly consistent with a continuous process. However, based on the forces associated to the impact process, increasing the number of modes, does not lead to consistent results. Figures 12 and 13 show the reaction at the revolute joint of the simulations with 10 and 15 mode shapes. As can be seen, the magnitude of the reactions is much greater in the solution provided by 15 mode shapes than in that obtained with 10 mode shapes.

6. SUMMARY AND CONCLUSIONS

In this work, the generalized impulse–momentum balance equations were used to simulate the impacts of rigid bodies on flexible beams of structures and mechanisms. The system of algebraic equations is the result of applying impulsive dynamics to flexible multibody systems, using the floating frame of reference approach. The coefficient of restitution is included in the formulation to account for the energy lost in the vicinity of the contact area. Friction is not considered. The flexible co-ordinates used to describe elastic displacements in the impacted beams can be the nodal co-ordinates of the finite element method or, alternatively, a set of eigenvectors numerically obtained from the finite element discretization.

From the analysis performed, the following conclusions can be drawn:

(1) The simulations show that, when a rigid body impacts a flexible beam, the equations of impulse–momentum balance have to be solved many times before the collision is concluded. As shown in this paper, this numerical procedure is unrelated with the real phenomenon of succession of impacts, which occurs in the impact of flexible bodies when the collision involves several periods of contact between the surfaces. The reason for these many balances during the collision is that the rigid body, with a mass of the same order of magnitude as the flexible body, collides directly on the node at the contact section. However, the mass associated to this contact section is much smaller than that of the whole flexible beam.

(2) The number of balances increases as the number of flexible degrees of freedom does, at the expense of a decreased intensity in instantaneous impacts. This is a consequence of the mass associated to the contact section being reduced when the geometric discretisation is refined.

(3) As a result of this succession of balances, the coefficient of restitution loses its physical significance because there can never be as many real contact periods as balances solved. Hence, the numerically simulated phenomenon lacks physical interpretation.

(4) Numerically, using a coefficient of restitution smaller than one can lead to final relative velocities for the impacted bodies even higher than the relative velocities obtained with a unity coefficient of restitution. Moreover, integrations do not give consistent results with coefficients smaller than one, they exhibit a strong dependence on the time step. Satisfactory results are obtained with a unity coefficient of restitution.

(5) In addition, simulations for axial impacts are highly consistent with the analytical results for a unity coefficient of restitution. Convergence of the displacements due to the impact process in both axial and transverse impacts as the number of flexible co-ordinates is increased is excellent. However, the forces associated to the transverse impacts on rotating beams are not accurately obtained.

The analysis presented in this paper is concerned with impacts in which the rigid impactor has the same mass as the flexible body. The conclusions can be extended to impacts between rigid and flexible slender bodies with masses of the same order of magnitude at moderate impact velocities. However, it is important to note that the generalized impulse–momentum balance equations involving the coefficient of restitution can give accurate results when the mass of the impactor is much smaller than that of the flexible body. In this case, the impact can be solved in a single balance and the coefficient of restitution can be used to characterize the local energy loss.

ACKNOWLEDGMENT

This research was supported by Spain's Ministry of Education and Culture (Project reference PB94-1189-C02-01) and conducted in part at the Department of Mechanical Engineering of the University of Illinois at Chicago. The helpful assistance of Dr Ahmed A. Shabana is gratefully acknowledged.

REFERENCES

1. R. H. Wehage and E. J. Haug 1982 *Journal of Mechanical Design* **104**, 778–784. Dynamic analysis of mechanical systems with intermittent motion.
2. Y. A. Khulief and A. A. Shabana 1985 *ASME Paper* 84-*DET*, 116. Dynamic analysis of constrained systems of rigid and flexible bodies with intermittent motion.
3. A. S. Yigit, A. G. Ulsoy and R. A. Scott 1990 *Journal of Vibrations and Acoustics* **112**, 65–70. Dynamics of a radially rotating beam with impact, Part 1: theoretical and computational model.
4. A. S. Yigit, A. G. Ulsoy and R. A. Scott 1990 *Journal of Vibrations and Acoustics* **112**, 65–70. Dynamics of a radially rotating beam with impact, Part 2: experimental and simulation result.
5. H. Palas, W. C. Hsu and A. A. Shabana 1992 *Journal of Acoustics and Vibration* **114**, 364–373. On the use of momentum balance and the assumed modes method in transverse impact problems.
6. W. C. Hsu and A. A. Shabana 1993 *Journal of Sound and Vibration* **168**, 355–369. Finite element analysis of impact-induced transverse waves in rotating beams.
7. W. H. Gau and A. A. Shabana 1995 *Journal of Mechanical Design* **117**, 336–342. Use of the finite element method in the analysis of impact-induced longitudinal waves in constrained elastic systems.

8. K. H. HWANG and A. A. SHABANA 1995 *Journal of Sound and Vibrations* **186**, 495–525. Effect of mass capture on the propagation of transverse waves in rotating beams.
9. A. S. YIGIT and A. P. CHRISTOFOROU 1995 *DE-Vol*. 84–3, *Design Engineering Technical Conferences*, *Vol*.3-*Part C*, *ASME*. The efficacy of the momentum balance method in transverse impact problems.
10. A. A. SHABANA 1989 *Dynamics of Multibody Systems*. New York: Wiley.
11. A. E. H. LOVE 1944 *A Treatise on the Mathematical Theory of Elasticity*. New York: Dover.
12. W. GOLDSMITH 1960 *Impact*, *the Theory and Physical Behaviour of Colliding Solids*. London: Arnold.
13. S. P. TIMOSHENKO and J. N. GOODIER 1970 *Theory of Elasticity*. New York: McGraw-Hill; 3rd edition.
14. A. S. YIGIT and A. P. CHRISTOFOROU 1997 *First Symposium on Multibody Dynamics and Vibrations*, DETC97/VIB-4208, ASME. Effect of flexibility in transverse impact problems.
15. J. L. ESCALONA, J. MAYO and J. DOMÍNGUEZ 1997 *First Symposium on Multibody Dynamics and Vibrations*, DETC97/VIB-4207. ASME. New numerical method for the dynamic analysis of impact loads in flexible beams.
16. D. STOIANOVICI and Y. HURMUZLU 1996 *Journal of Applied Mechanics* **63**, 307–316. A critical study of the applicability of the rigid body collision theory.
17. K. J. BATHE 1996 *Finite Element Procedures*. Englewood Cliffs, NJ: Prentice-Hall.
18. A. A. SHABANA 1986 TR No. 86–3. User's Guide to DAMS. Department of Mechanical Engineering, University of Illinois at Chicago, Chicago, IL.